

# Thermotropic Liquid Crystals in Polypeptides with Mesogenic Side Chains. 1

Junji Watanabe\* and Toshihiko Tominaga

Department of Polymer Chemistry, Tokyo Institute of Technology,  
Ookayama, Meguro-ku, Tokyo 152, Japan

Received November 13, 1992

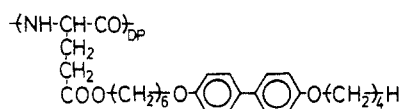
**ABSTRACT:** We prepared a new type of thermotropic liquid crystalline polypeptide, denoted PLG-BP-64 (see text), in which mesogenic biphenyl moieties are linked to a mesogenic  $\alpha$ -helical main chain with a flexible spacer. This polymer exhibits transitions at  $T_1 = 143^\circ\text{C}$  and  $T_2 = 222^\circ\text{C}$  and forms three distinct phases, the crystalline, the smectic A, and the cholesteric phases. In the crystalline phase below  $T_1$ ,  $\alpha$ -helical main chains form the layered structure and the biphenyl moieties in the side chains are crystallized in the space between the layers with their long axes perpendicular to the layer. In the temperature range from  $T_1$  to  $T_2$ , the layered structure remains unchanged but the biphenyl moieties are in a liquid crystalline state in which the molten biphenyl groups are located still having the orientational order between the main-chain layers as in the crystalline phase. The structure can be assigned to be the smectic A phase. At the final temperature stage above  $T_2$ , the layered structure collapses and the biphenyl moieties are randomly dispersed around the main chain, which results in the well-known cholesteric phase based on the  $\alpha$ -helical mesogenic groups. The thermotropic transition behavior and the mesophase structures are illustrated by considering a coupling effect of main-chain and side-chain mesogenic groups.

## Introduction

There is considerable interest in side-chain liquid crystalline (LC) polymers because the chemical structure can be varied in numerous ways to influence the mesophase structure and properties. In these polymers, the monomeric mesogen appears as a pendant group attached to the main chain by a flexible spacer. This type of connection preserves the delicate interactions between the pendant mesogenic moieties by decoupling the motion of the main chain from that of the pendant group. Most of the side-chain LC polymers that have been prepared to date have contained polysiloxane, polyacrylate, or polymethacrylate main chains. Detailed reviews<sup>1-3</sup> have appeared, laying stress upon the roles of the flexibility of the main chain, the length of the spacer, and the kind of mesogenic group on the thermotropic phase behavior and the liquid crystalline structure.

On the other hand,  $\alpha$ -helical polypeptides comprise an important class of polymers that can form liquid crystals owing to their hard-rod shape. The discovery of thermotropic polypeptides by our research group<sup>4-12</sup> has increased the interest in liquid crystals of hard-rod molecules. The thermotropic polypeptides have been prepared by attaching long alkyl side chains, and cholesteric, smectic, and columnar liquid crystals have been observed with definitive experimental evidence.

In this paper, we prepared another type of thermotropic polypeptide denoted PLG-BP-64 in which the mesogenic biphenyl moieties are linked to the mesogenic  $\alpha$ -helical polypeptide with a flexible spacer. In one aspect, this polymer can be regarded as a kind of side-chain LC polymer, but in another aspect it can be considered as a rigid rod main-chain LC polymer. Thermotropic liquid crystal behavior of this polymer will be described through DSC, optical microscopic, and X-ray observations.



PLG-BP-64

## Experimental Section

**Materials.** 4-Butoxy-4'-(( $\omega$ -hydroxyhexyl)oxy)biphenyl (BH-BHP) employed as a mesogenic side-chain group was prepared by the following procedure. First, 4-butoxy-4'-hydroxybiphenyl was synthesized by standard methods from 4,4'-biphenyldiol with bromobutane in the presence of sodium hydroxide. The crude products were purified via the sodium salt, which is soluble in hot water and can be recrystallized from ethanol. 4-Butoxy-4'-hydroxybiphenyls (0.1 mol) were dissolved in 150 mL of hot ethanol, and 0.11 mol of potassium hydroxide in 30 mL of water was added under stirring.  $\omega$ -Chlorohexanol (0.11 mol) was added, and the mixture was refluxed for 20 h. After the solution was diluted with an equal volume of water, ethanol was distilled off. The resultant precipitate was filtered and washed with hot potassium hydroxide solution and water. The dry BH-BHP products were recrystallized from ethanol. BH-BHP exhibits a single transition of crystal melting and so forms no liquid crystal. The melting temperature as determined by DSC is  $148^\circ\text{C}$ .

The PLG-BP-64 was prepared by an ester exchange reaction between 1 g of poly( $\gamma$ -methyl L-glutamate) (PMLG) and 10 g of BH-BHP. The reaction was carried out in 1,2-dichloroethane using *p*-toluenesulfonic acid as a catalyst at  $60^\circ\text{C}$ . Reaction for 10 days is necessary for perfect ester exchange, which was confirmed from elimination of the NMR signal assigned to the methyl group of the PMLG side chain<sup>5</sup> and also from a quantitative assignment of the NMR signal due to the biphenyl group of the BH-BHP side chain. Two kinds of PLG-BP-64 with different degrees of polymerization (DP) were prepared from PMLG, PLG-BP-64(700) and PLG-BP-64(70), with DPs of 700 and 70, respectively. Film specimens were cast from chloroform solutions and annealed at  $150^\circ\text{C}$  for 30 min prior to the measurements.

**Methods.** DSC measurements were performed with a Perkin-Elmer DSC-II calorimeter at a scanning rate of  $10^\circ\text{C}/\text{min}$ . Wide-angle X-ray diffraction patterns of the polymers were recorded with a flat-plate camera mounted to a Rigaku-Denki X-ray generator emitting Ni-filtered Cu K $\alpha$  radiation. The temperature of the sample was controlled by placing the sample in a Mettler FP-80 hot stage mounted in the beam path. The film to specimen distance was determined by calibration with silicon powder. Optical microscopic observations of the liquid crystalline textures were made with an Olympus BH-2 polarizing microscope equipped with a Mettler FP-80 hot stage.

## Results

Figure 1 shows DSC curves of PLG-BP-64(700) film obtained for consecutive heating and cooling cycles. In

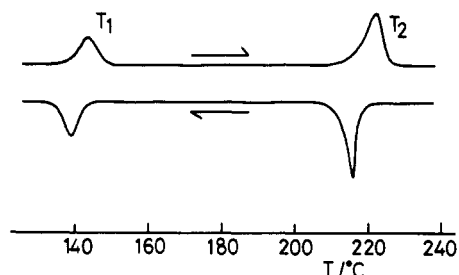


Figure 1. DSC thermograms of PLG-BP-64(700) film.

Table I. Transition Temperatures (°C) and Enthalpy Changes (kcal/mol; in Parentheses) of Polymers

|                | $T_1$        | $T_2$        |
|----------------|--------------|--------------|
| PLG-BP-64(700) | 143<br>(0.4) | 222<br>(0.7) |
| PLG-BP-64(70)  | 119<br>(0.6) | 164<br>(1.0) |

the first heating, endothermic peaks are seen at  $T_1 = 143$  °C and  $T_2 = 222$  °C. Upon cooling, the corresponding transitions are observed at  $T_1 = 139$  °C and  $T_2 = 216$  °C. The fundamental data related to the transitions are listed in Table I.

Optical microscopy revealed no fluidity and no typical texture at temperatures below  $T_1 = 143$  °C. At  $T_1$  the onset of melting occurs and so mechanical displacement of the coverslip becomes easy. In this phase, strong birefringence is observed as in the preceding phase. At  $T_2 = 222$  °C, the material begins to flow spontaneously and at the same time the birefringence becomes substantially weak although it still persists over the whole domain. In this phase, a fingerprint texture can be observed as shown in Figure 2a, indicating that a cholesteric liquid crystal is formed as has been observed so far in thermotropic polypeptides.<sup>6</sup> The cholesteric phase is invariably observed up to 250 °C, at which decomposition significantly occurs. On cooling the cholesteric phase to temperatures below  $T_2 = 216$  °C, the highly birefringent phase reappears as pseudobatonnets (see Figure 2b), which finally change to an uncertain texture (see Figure 2c). At  $T_1 = 139$  °C, mechanical displacement of the coverslip becomes impossible, indicating that the material reenters into the solid phase. Both DSC and optical microscopic observations thus indicate three distinct phases, which can be assigned to be the crystalline, smectic A, and cholesteric phases as presented later.

The low-molecular-weight material, PLG-BP-64(70), also indicates two transitions, the temperatures of which are lower than those of the high-molecular-weight PLG-BP-64(700) as shown in Table I. Phase transitions similar to those in PLG-BP-64(700) are detected by optical microscopy except that the cholesteric phase coexists with the isotropic phase in the final temperature range above  $T_2$  (see Figure 3).

The X-ray pattern was observed for each phase in PLG-BP-64(700). Here, the observation was performed for the fiber specimen that was prepared by stretching the cholesteric phase at 230 °C. For this fiber specimen, the 1.5-Å reflection can be observed just on the meridional line, indicating that the component polypeptide assumes an  $\alpha$ -helical conformation with its helical axis parallel to the fiber axis.<sup>13</sup>

At room temperature, the X-ray pattern shows several well-defined reflections (Figure 4a). The lattice spacings of the reflections are listed in Table II. In this pattern, there are two basic features to note: (1) the small-angle reflections and (2) the wide-angle reflections. All the small-

angle reflections are located on the equator and hence can be attributed to the lateral packing of  $\alpha$ -helices. The two-dimensional unit cell based on these reflections was uniquely determined to have lattice parameters of  $a = 30.9$  Å,  $b = 14.3$  Å, and  $\gamma = 103.3^\circ$  (see Table II). This unit cell, illustrated in Figure 5, can be characterized by the large value of  $a$  and the small value of  $b$ , indicating that the polymer molecules are appreciably deformed from a cylindrical shape to construct the layered structure. Here, the layer is formed along each (100) plane. Although the X-ray data offer no information on the packing of  $\alpha$ -helices along their chain axes, we can calculate a density of 1.17 g/mL by considering the repeat length of 1.5 Å of the  $\alpha$ -helix. This value is in good agreement with the observed one, 1.16 g/mL.

In the wide-angle region, three distinct reflections are observed with different azimuthal angles (see Figure 4a). From their Bragg spacings and diffraction geometries, these can be assigned to the two-dimensional lattice with  $a' = 8.46$  Å,  $b' = 5.13$  Å, and  $\gamma' = 90^\circ$ , in which the  $a'$  and  $b'$  axes lie parallel and perpendicular to the  $\alpha$ -helix axis, respectively. This lattice resembles the subunit cell that is attained by  $c$  projection of the monoclinic unit cell ( $a = 8.12$  Å,  $b = 5.63$  Å,  $c = 9.51$  Å, and  $\beta = 95.1^\circ$ ) in the crystal structure of biphenyl,<sup>14,15</sup> indicating that the side-chain biphenyl moieties are in a crystalline state. Figure 6 illustrates the packing of biphenyl moieties into an observed two-dimensional lattice. Here, two biphenyl groups are included in the unit cell, and their spatial orientation is illustrated according to the  $P2_1/a$  space group in the biphenyl crystal.<sup>15</sup>

It is thus obvious that the material at room temperature is essentially crystalline in character. In Figure 7, the overall crystalline structure is illustrated by combining two lattices such that the side-chain crystals are included in the space between the layers of the main chains. Here, the side chains from one layer protrude in the opposite direction so as to fill the space on either side of the layers. On the other hand, the side chains from neighboring layers interpenetrate each other, and the biphenyl moieties are placed in the central part between the layers with their long axis perpendicular to the layers. Such an association of side chains can be supported from the fact that the layer spacing approximates the length of the side chain in an extended form. A similar combined crystalline structure has been observed in poly( $\gamma$ -alkyl L-glutamate)s with long alkyl side chains.<sup>5</sup>

It is interesting to show that in this crystalline structure the  $\alpha$ -helical conformation can offer an optimum site for crystallization of the biphenyl groups and so every biphenyl group is able to participate in crystallization. Figure 7c illustrates the projection of molecules on a plane perpendicular to the layer which corresponds to the axial projection with respect to the side-chain biphenyl groups. According to this projection, we can estimate the number of side chains passing through a unit area defined by the repeating length (27 Å) of the  $\alpha$ -helix<sup>16</sup> and the distance (14.3 Å) between molecules along the layer (refer to Figure 7c). The size of the crystal lattice of biphenyl groups elucidated above dictates that the number of biphenyl groups is approximately 18. This number is exactly equal to the number of side chains that should be located in a unit area.<sup>13,16</sup> Thus, the crystallization of side chains does not require a distortion of main-chain conformation but only a gathering of side chains into a space between the main-chain layers.

On heating to temperatures above  $T_1$ , the small-angle equatorial reflections undergo no essential change while

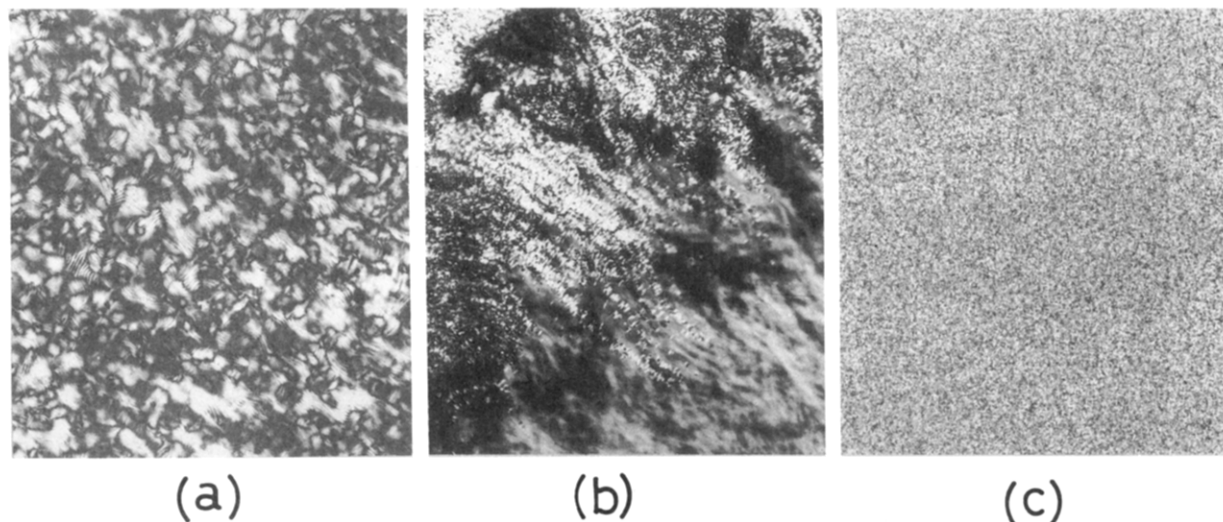


**Figure 2.** Optical microscopic textures of PLG-BP-64(700): (a) fingerprint texture observed in the cholesteric phase at 240 °C; (b) pseudobatonnets of the smectic A phase appearing on cooling the cholesteric phase to 216 °C; (c) uncertain texture of the smectic A phase observed at 150 °C.

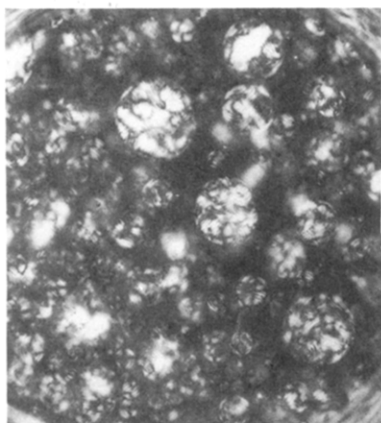


**Figure 3.** Optical microscopic texture observed for PLG-BP-64(70) at 230 °C. The texture indicates the coexistence of the cholesteric and isotropic phases.

the sharp wide-angle reflections disappear and are replaced by a simple broad reflection of 4.5 Å with relatively strong intensity on the meridional line as found in Figure 4b and Table II. In this phase, hence, the crystallites of biphenyl moieties undergo a melting although the main chains are still packed to form the layer. The two-dimensional lattice in the main-chain packing has the lattice constants  $a = 31.1$  Å,  $b = 15.0$  Å, and  $\gamma = 104.0^\circ$ . In a comparison with the lattice parameters in the crystalline phase, it can be found that the layered structure is not essentially changed; only a negligible increase of the constant  $a$  from 30.9 to 31.1 Å and a small increase of the constant  $b$  from 14.3 to 15.0 Å can be seen. Thus, the biphenyl moieties in the molten state are still located between the main-chain layers and may be packed with their long axes perpendicular to the layers because of their limited available space as in the crystalline phase. This means that the biphenyl moieties are in a smectic A liquid crystalline state. The liquid crystalline arrangement of biphenyl moieties can be supported from the facts that the strong birefringence of the crystalline phase is invariably observed in this phase and that the 4.5-Å reflection associated with the average lateral spacing between the biphenyl groups is consistent with most values reported so far for smectic A phases.<sup>17</sup> The overall structure of this smectic A phase is illustrated in Figure 8a. This structure is similar to the smectic A phase observed in conventional side-chain LC polymers<sup>18–22</sup> although it is remarkable that the main-chain  $\alpha$ -helices

are located at the confined position so as to form the layered structure by themselves.

In the cholesteric phase appearing on heating above  $T_2$ , all sharp reflections disappear, leaving a broad reflection with a spacing around 24 Å (see Figure 4c and Table II). In this phase, hence, the layered structure collapses completely. Further, a remarkable decrease of the birefringence indicates the loss of the orientational order in the side-chain biphenyl moieties. In fact, the spacing of 24 Å approximates the average diameter of a molecule that is expected when the side chains are randomly displaced around the  $\alpha$ -helical main chain. The cholesteric phase, hence, is concluded to result simply from the main-chain mesogens as has been observed in poly-(L-glutamates).<sup>5–12</sup> The biphasic appearance of the cholesteric and isotropic phases in the lower molecular weight PLG-BP-64(70) further reinforces this conjecture since it can be caused by the reduced axial ratio of the main-chain  $\alpha$ -helix.<sup>23</sup> The cholesteric structure is schematically illustrated in Figure 8b.

## Discussion

In this study, we have treated a new type of thermotropic liquid crystalline polypeptide with a comblike structure including the main-chain and side-chain mesogens and have found the following phase transitions:



In the crystalline and smectic A phases, the molecules construct the characteristic layered structure in which the  $\alpha$ -helical main chains form the layer and the side-chain mesogenic groups are placed in the central part of the layers with their long axes perpendicular to the layer. In the crystalline phase, the side-chain mesogens are in a crystalline form while in the smectic A phase they are in a molten state. The cholesteric phase produced by the main-chain  $\alpha$ -helices appears following the collapse of the layered structure.

First, we consider these transitions by laying stress upon the side-chain mesogens. With respect to the side-chain mesogens, the above-mentioned transitions can be illus-

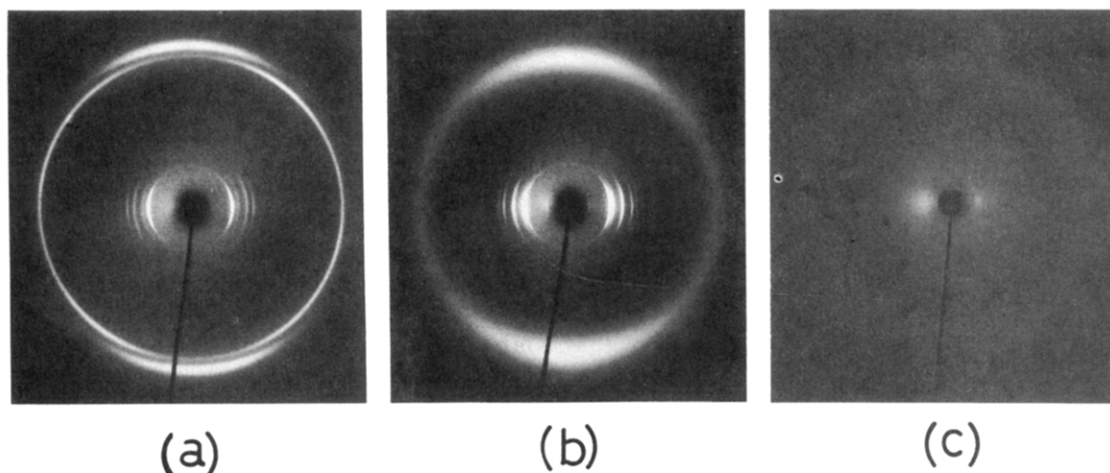


**Figure 4.** X-ray pattern observed for PLG-BP-64(700) fiber: (a) crystalline phase at room temperature; (b) smectic A phase at 150 °C; (c) cholesteric phase at 230 °C. The fiber axis is in the vertical direction.

**Table II.** X-ray Data of PLG-BP-64(700)

| crystalline phase<br>(at 20 °C) |             |         | smectic A phase<br>(at 150 °C) |             |         | cholesteric phase<br>(at 230 °C) |
|---------------------------------|-------------|---------|--------------------------------|-------------|---------|----------------------------------|
| $d_0$ (Å)                       | $d_c^a$ (Å) | $hkl^a$ | $d_0$ (Å)                      | $d_c^a$ (Å) | $hkl^a$ | $d_0$ (Å)                        |
| Small-Angle Region              |             |         |                                |             |         |                                  |
| 30.1 (vw)                       | 30.04       | 100     | 30.2 (vw)                      | 30.16       | 100     | ~ 24 (s)                         |
| 15.0 (s)                        | 15.02       | 200     | 15.1 (s)                       | 15.08       | 200     |                                  |
| 13.6 (w)                        | 13.87       | 010     | 14.5 (vw)                      | 14.56       | 010     |                                  |
| 11.6 (m)                        | 11.62       | 110     | 12.1 (m)                       | 12.02       | 110     |                                  |
| 10.0 (m)                        | 10.01       | 300     | 10.1 (m)                       | 10.05       | 300     |                                  |
| 9.18 (vw)                       | 9.19        | 210     | 9.39 (vw)                      | 9.40        | 210     |                                  |
| 7.45 (w)                        | 7.51        | 400     | 7.51 (w)                       | 7.54        | 400     |                                  |
| 6.01 (vw)                       | 6.01        | 500     | 6.05 (vw)                      | 6.03        | 500     |                                  |
| Wide-angle Region               |             |         |                                |             |         |                                  |
| 4.40 (s)                        | 4.39        | 110     | ~ 4.5 (m)                      |             |         |                                  |
| 4.24 (s)                        | 4.23        | 200     |                                |             |         |                                  |
| 3.27 (m)                        | 3.26        | 210     |                                |             |         |                                  |

<sup>a</sup> Indices and  $d_c$  are based on the unit cells cited in the text.

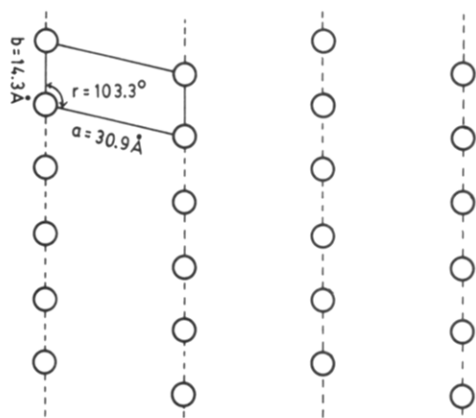
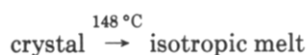


**Figure 5.** Illustration for the packing of  $\alpha$ -helices in the crystalline phase projected along their helical axes. The  $\alpha$ -helices are packed into the layered structure with two-dimensional positional order.

trated as follows:



This transition behavior is interestingly compared with that of monomeric 4-butoxy-4'-(( $\omega$ -hydroxyhexyl)oxy)-biphenyl (BHHBP):



From this comparison, one can find that a distinct feature, an ability to form the smectic A phase, is newly induced

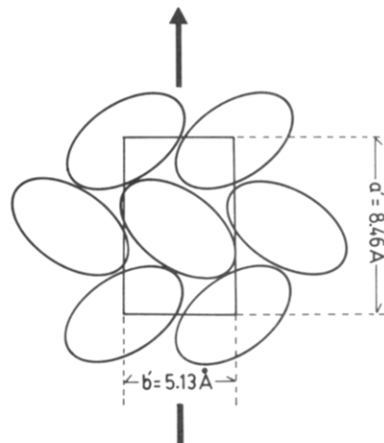


**Figure 6.** Illustration for the packing of side-chain biphenyl moieties projected along their long axes. Two biphenyl groups are included in a unit cell, and their spatial orientation is illustrated according to the  $P2_1/a$  space group in the biphenyl crystal. The arrow indicates the axis of the main-chain  $\alpha$ -helix.

for the mesogenic BHHBP in side chains although the crystal melting for both occurs at similar temperatures (148 °C for monomeric BHHBP and 143 °C for BHHBP in the side chain). This new distinct feature is hence obvious to result from the combined effects in which the  $\alpha$ -helical main-chain mesogens interact with the side-chain mesogens.

When the layered structure of the crystalline phase in Figure 7 is examined, one of the significant combined

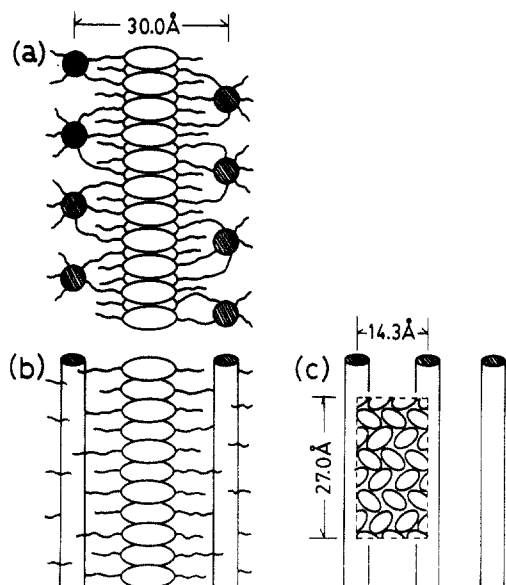


**Figure 7.** Proposed layered structure for the crystalline phase of PLG-BP-64(700): (a) viewed parallel to the chain axes of the  $\alpha$ -helices; (b) viewed parallel to the layer and perpendicular to the chain axes of the  $\alpha$ -helices; (c) viewed perpendicular to both the layer and the chain axes of the  $\alpha$ -helices.

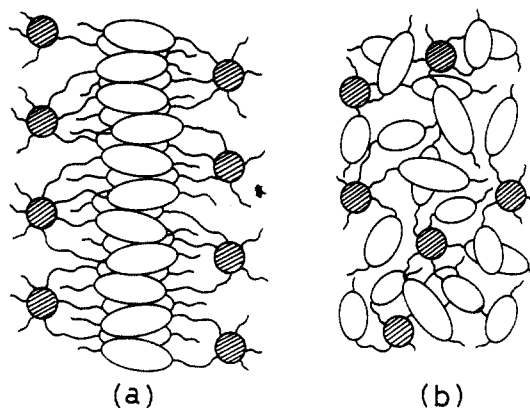


**Figure 8.** Illustration of (a) the smectic A layered structure and (b) the cholesteric structure projected along the  $\alpha$ -helical axis.

effects is a trend in which the side chains are segregated from the main-chain domains. Such a layered segregation structure may be caused primarily by the difference in chemical constitution between the main-chain and side-chain mesogens. Several segregation structures, spherical, cylindrical, and layered lamellar structures, are possible as have been elucidated in binary block copolymer systems.<sup>24,25</sup> In this case, however, the layered segregation structure would be the most preferential among them since only this type of segregation structure can effectively accommodate each mesogen into an anisotropic domain. An interesting thing is that the layered segregation structure is completely retained even after the side-chain crystals melt. This means that the enthalpic interaction energy to stabilize the segregation structure is large enough to overcome the entropic conformational energy which would facilitate the isotropic melting of side-chain mesogens. The molten side chains, thus, can use only a limited space as in the crystalline phase so that they retain the orientational order of the long axes and also the positional order along their long axes. This is a reason why the smectic nature has been newly attached to the side-chain BHHBP mesogens. On the other hand, the cholesteric phase which appears following the collapse of the layered structure can be simply understood as being produced by

a mutual miscibility of the main-chain and side-chain mesogens.

Among these phases, the smectic A phase is interesting and can be compared with that observed in conventional side-chain LC polymers. In conventional side-chain LC polymers, the question of the conformation of the flexible main chains has become a central issue. From X-ray measurements, it is assumed that in the aligned smectic phase the main chain is strongly confined between the mesogenic layers.<sup>18</sup> Small-angle neutron scattering on mixtures of unlabeled and labeled polymers has also exhibited that in several cases the backbone adopts an oblate conformation in the smectic A phase.<sup>19–22</sup> This has been understood by considering the confinement effect exerted by the smectic field on the main chain. The existence of the smectic A phase usually proceeds from the tendencies of the aromatic and aliphatic moieties to segregate so that the main chain should be preferentially located in the aliphatic part of the smectic layers. The present smectic A phase mimicking the distinct segregation structure is considered to be an extreme case of this. Here, it should be noted that in the present smectic A phase the main chains are totally packed with two-dimensional positional order. This brings up the simple question of whether the present smectic A phase is truly equivalent or not to the smectic A phase of conventional side-chain polymers, since we know that in the latter there can be seen only one-dimensional positional order along the director with respect to the mesogenic side-chain groups. This interesting question warrants further investigation.

## References and Notes

- Finkelmann, H.; Rehage, G. *Adv. Polym. Sci.* **1984**, *60/61*, 99.
- Shibaev, V.; Plate, N. A. *Adv. Polym. Sci.* **1984**, *60/61*, 173.
- McArdle, C. B., Ed. *Side-Chain Liquid Crystal Polymers*; Blackie, Chapman and Hall: New York, 1989.
- Watanabe, J.; Fukuda, Y.; Gehani, R.; Uematsu, I. *Macromolecules* **1984**, *17*, 1004.
- Watanabe, J.; Ono, H.; Uematsu, I.; Abe, A. *Macromolecules* **1985**, *18*, 2141.
- Watanabe, J.; Ono, H. *Macromolecules* **1986**, *19*, 1079.
- Watanabe, J.; Goto, M.; Nagase, T. *Macromolecules* **1987**, *20*, 298.
- Watanabe, J.; Nagase, T. *Macromolecules* **1988**, *21*, 171.
- Watanabe, J.; Nagase, T.; Itoh, H.; Ishi, T.; Satoh, T. *Mol. Cryst. Liq. Cryst.* **1988**, *164*, 135.
- Watanabe, J.; Nagase, T.; Ichizuka, T. *Polym. J.* **1990**, *22*, 1029.
- Watanabe, J.; Takashina, Y. *Macromolecules* **1991**, *24*, 3423.
- Watanabe, J.; Takashina, Y. *Polym. J.* **1992**, *24*, 709.
- Fraser, R. D. B.; MacRae, T. P. *Conformation in Fibrous Proteins*; Academic Press: New York, 1973.
- Hargreaves, A.; Rizvi, S. H. *Acta Crystallogr.* **1962**, *15*, 365.
- Trotter, J. *Acta Crystallogr.* **1961**, *14*, 1135.
- The  $\alpha$ -helix makes 5 turns by 18 residues. Along the helical axis, the height per residue is 1.5 Å and hence the true repeat length of the  $\alpha$ -helix is 27 Å (=1.5 Å  $\times$  18).
- Gray, G. W.; Goodby, J. W. F. *Smectic Liquid Crystals*; Leonard Hill: Glasgow and London, 1984.
- Davidson, P.; Levelut, A. M. *Liq. Cryst.* **1992**, *11*, 469.
- Keller, P.; Carvalho, B.; Cotton, J. P.; Lambert, M.; Moussa, F.; Peppy, G. *J. Phys., Lett.* **1985**, *46*, L1065.
- Noirez, L.; Cotton, J. P.; Hardouin, F.; Keller, P.; Moussa, F.; Peppy, G.; Strazielle, C. *Macromolecules* **1988**, *21*, 2889.
- Ohm, H. G.; Kirste, R. G.; Oberthur, R. C. *Makromol. Chem.* **1988**, *189*, 1378.
- Kalus, J.; Kostromin, S. G.; Shibaev, V. P.; Kunchenko, A. B.; Ostanevich, Yu. M.; Svetogorsky, D. A. *Mol. Cryst. Liq. Cryst.* **1988**, *155*, 347.
- Flory, P. J. *Proc. R. Soc. London* **1956**, *A234*, 60.
- Henke, C. S.; Thomas, E. L.; Fetters, L. J. *J. Mater. Sci.* **1968**, *23*, 1685.
- Thomas, E. L.; Anderson, D. M.; Henke, C. S.; Hoffman, D. *Nature* **1968**, *334*, 598.